Adam Mickiewicz University in Poznań

Faculty of Physics

Individual Project: Designing a Velocity Prediction Program for the Formula Windsurfing Foil Class with optimization

Author:
Oliwier Urbański
oliwier1459@gmail.com

Faculty Advisor:
Professor Tomasz T. Polak
tppolak@amu.edu.pl

ABSTRACT Implementation of hydrofoils in the Formula Windsurfing turned setting the gear into an even more intricate physical problem. Multiplicity of adjustable parameters like the rear wing angle, rake angle, position of the straps, mast foot, downhaul tension, position and length of the harness lines, height of the boom and many more, gives sailors a real challenge. Due to the high dimensionality of this parameter space, an enormous number of combinations must be tested before finding the optimal one. Thus a Velocity Prediction Program enabling optimization may be very helpful. This paper is focused on creating such a program (which is implemented in Mathematica) and explaining its details. It takes into account the nontrivial geometry of the sailor body and the sail (not present in similar programs designed for boats), which results in a model with ten degrees of freedom. Simple engineering mathematical formulas are used to describe the aero-hydrodynamic forces to produce only qualitatively reasonable outputs. Ultimately, the program is meant to be filled with accurate CFD data and used for optimizing real-life windsurfing gear. Attention is also paid to the numerical methods needed for finding balance and optimizing performance. Finally, generated polar plots are presented and qualitatively discussed.

I. MOTIVATION

A certain foiling windsurfer is sailing upwind, highly focused on handling the gear, so as to fly with optimal speed and angle. Unexpectedly, another competitor appears on his windward side, screens the wind and easily overtakes the former. However, the faster sailor is not able to keep the angle of the slower, so it is not obvious who performs better. These two setups are like different units: even though both sailors are optimizing their velocity made good, they do not have the same speed and true wind angle. This is just an exemplary situation, but such discrepancies are common in the Formula Windsurfing Class. In severe cases, two racers may have no opportunity to compete by means of sailing strategy because of significant disproportion in velocity made good. Equipment (with multiple adjustable parameters), physical features of the sailor and his technique are the factors responsible for that. Testing every possible setting on the water is forbiddingly time-consuming, so this paper aims at developing a Velocity Prediction Program, which can be used for optimization of real-life windsurfing gear, after feeding it with CFD data.

II. IDEA OF POLAR PLOTS

Most important information about yacht performance is presented on a polar plot. Let v_T be the true wind speed and $\varphi \in [0, \pi]$ denote an angle between directions of v_T and yacht speed v, with $\varphi = 0$ representing going directly upwind and $\varphi = \pi$ - directly downwind. Function $v(v_T, \varphi)$, for a given value of v_T, can be plotted in polar coordinates (v, φ), which constitutes a polar plot. It can be used to determine most relevant quantities. For example, velocity made good in sailing upwind is found as $\max_{\varphi\in[0,\pi]} v(\varphi)\cos\varphi$, while for sailing downwind it is $-\min_{\varphi\in[0,\pi]} v(\varphi)\cos\varphi$. Thus theoretical prediction of polar plots for a considered sailing unit is a major task in the physics of sailing. Here we are interested in the special case of windsurfing foil.

In order to familiarize with the concept of a polar plot, it is illuminating to invoke a well-known example of an ice-boat, described for example in [3] and [4]. Among all sailing units, land-yachts and ice-boats experience minimal resistance (i. e. non-aerodynamic force opposing aerodynamic thrust). It turns out, that even in the absence of any resistance, finite speed is achieved. As argued in [3], ice-boats are often close to this limiting case. The mechanism responsible for that can be most clearly demonstrated on a wind diagram (fig. 1). v_A denotes speed of the apparent wind (i. e. air motion which is measured in the rest frame of the sail) and α is the apparent wind angle. For fixed v_T and φ, α decreases as the unit speeds up (v increases). It means that for sufficiently high v, apparent wind blows almost directly from the bow and sail is unable to produce any thrust, thus limiting final velocity. If no resistance is present, ice-boat

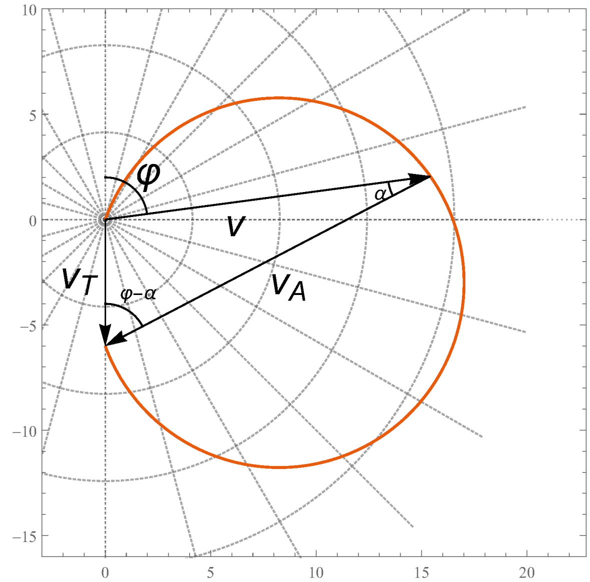

Figure 1: Theoretical polar plot of an ice-boat

reaches equilibrium when zero thrust is produced. This happens for a particular angle α, which depends on the efficiency of the sail and on windage (aerodynamic drag, which as explained before, is excluded from "resistance"). For this reason, polar plot is fully determined just by a simple condition $\alpha = \text{const}$. According to the inscribed angle theorem, curve given by coordinates (v, φ) is a circle (fig. 1). In order to obtain functional form of dependence $v(v_T, \varphi)$, the law of sines can be used:

$$\frac{v}{\sin(\varphi - \alpha)} = \frac{v_A}{\sin\varphi} = \frac{v_T}{\sin\alpha} \tag{1}$$

$$v(v_T, \varphi) = v_T \frac{\sin(\varphi - \alpha)}{\sin\alpha} \tag{2}$$

Example of the ice-boat is the only one, which can be summarized sensibly by a closed-form formula (2). Nevertheless, equations (1) and (2) are applicable in general, but angle α is no longer constant in the presence of significant resistance and has to be replaced by some function $\alpha(v_T, \varphi)$.

Ordinary yachts have quite different polar plots (fig. 2), determined mainly by resistance (i. e. achieved speeds are far from the limit dictated by apparent wind as for ice-boats). Foiling units experience significantly smaller resistance, which makes their polar plots more similar to those of ice-boats (fig. 3). For both, angle α remains acute for all practical angles φ (which is in general a feature of high-speed sailing). This forces the sail to stay almost in the same position in sailing upwind, as well as in sailing downwind. For mentioned reasons, it is possible to come across the opinion that windsurfing foil is an "ice-boat on water". However, as further results will reveal, even foilers are still far from the limit almost met by ice-boats.

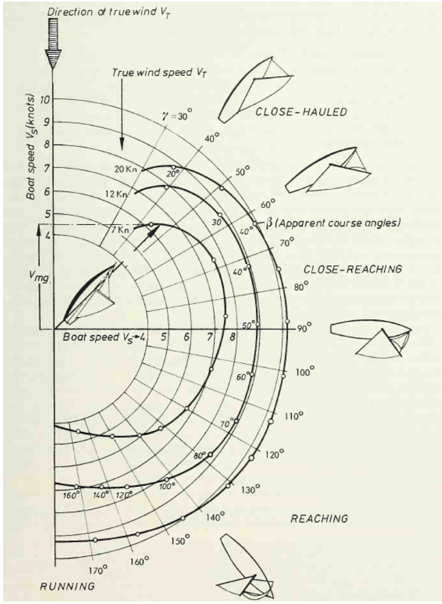

Figure 2: Polar plots for the 12-meters yacht, taken from [3]

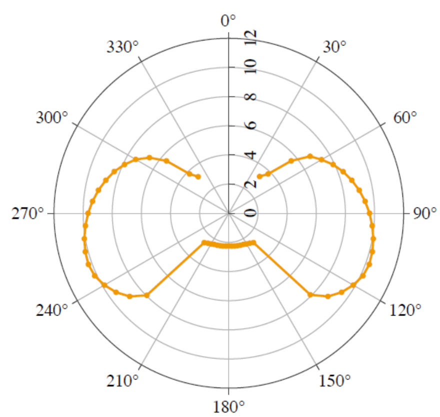

Figure 3: Theoretically predicted polar plot for the International Moth, taken from [4]

III. INTUITIONS BEHIND THE VPP

In this section we will propose a rough idea for constructing polar plots for windsurfing foil. Complexity which we are about to encounter, makes this task impossible to solve by means of a single formula, as in the case of an ice-boat. Rather, a special program called VPP (Velocity Prediction Program) is needed.

Sailing on course can be treated as a static situation, so in order to determine the state of the unit, we seek for equilibrium in which all forces and torques balance. Even in presence of waves or small gusts, we can speak about time-averaged forces and still follow the same approach. Figure 4 depicts famous foiler Nicolas Goyard during a slalom race, with added arrows representing the most important forces. They are classified as follows:

Figure 4: Forces acting on a windsurfing foil set in action. Original photo taken from the PWA official website `https://www.pwaworldtour.com/index.php?id=2254&tx_pwagallery_pi1%5BcurrentPage%5D=17&cHash=8753f80c75317880a968b8379cc1ad55`

- Aerodynamic forces:
  1. sail thrust
  2. sail side force
- Gravity forces:
  3. weight
- Hydrodynamic forces:
  4. main lift
  5. lateral force
  6. drag

For a rigid body, we expect six equations (three components of the net force and other free components of the net torque). Here, however, the situation is even more complicated, because the board (with foils), sail and sailor may change their relative orientation. This in the worst case would triple the number of equations. Luckily, these three parts exert some forces and torques on each other, in a way, that allows us to reduce complexity. The windsurfer is connected with the board by his feet at two points. Front foot can be assumed to be always in the foot strap. Thus the board and the sailor may exert force on each other in all directions. In the case of torque, windsurfer cannot apply any significant torque (measured with respect to the front strap) parallel to the line joining his feet (otherwise it would be uncomfortable to maintain for longer time). In the remaining two linearly independent directions there is no problem in applying torque. If the sail is regarded (or actually the entire rig), it is connected with the board by a rubber joint, which transfers any force freely, but no torque (with respect to that joint). Of course, the sailor exerts force and torque on the sail, but it is done in a special way and we are going to keep this interaction as variables describing state of the foil and thus not reducing more equations. Summarizing, we are left with six equations for the force-torque balance of the entire system, one equation for torque balance of the sailor and three equations for torque balance of the sail. This results in ten equations in total. Now we need to find at least ten variables that describe state of the foil during a flight, in order to obtain solvable system of equations.

Here we have to distinguish between state variables and equipment parameters. The former may change during sailing and describe current state of the foil in a flight. The later express equipment setup and are not varied during sailing, thus we regard them temporarily as constant. Quantities v_T and φ deserve separate classification, as for each possible pair of them we try to calculate performance. Therefore they will be referred to as input variables.

Total number of state variables is greater than ten. This allows the sailor to ride differently for the same input variables. However, this freedom is somehow constrained and sailors usually adopt one, most efficient technique. For this reason, among all state variables, we can further distinguish ten basic (which we treat as unknowns in the ten equations for equilibrium) and a few additional variables corresponding to the mentioned freedom in performance.

Choice of equipment parameters (not their values, but what they should represent) is quite natural, because they are already specified clearly enough by sailors and manufacturers. The case of state variables is harder, because they can be picked in a number of ways. Choosing ten basic out of them is another dilemma. In order to do it reasonably, sailing intuition has been used: Additional variables should correspond to elements directly controlled by the sailor. These are: bending knees (described by effective lengths of the legs), position of the rear foot (which is often out of strap), height of the flight and outhaul regulation. Remaining (basic) state variables are: speed of the foil, three angles describing orientation of the sail, next three angles describing orientation of the board, one angle corresponding to long-wise shift of sailor's body (it is not directly under windsurfer's control, because it is determined by the torque from the foils), tension of the harness lines and one component of torque exerted by sailor's arms through the boom on the sail.

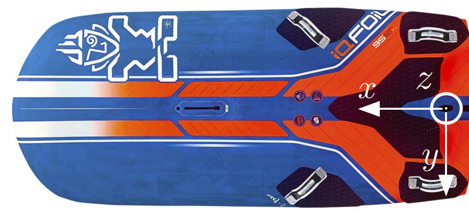

Figure 5: Board coordinate system shown on the Olympic iQFOiL model

IV. MODULAR STRUCTURE OF THE VPP

Before we can solve the ten equations for equilibrium of the foil, they need to be first established. This requires knowledge of the aerodynamic and hydrodynamic forces and torques involved. Such a task is quite difficult on its own and is usually completed by collecting data from experiments or CFD (computational fluid dynamics) simulations. Future VPP should be able to take in such data, and generate appropriate polar plots. For this reason, it is convenient to built the VPP from modules - parts of code which are responsible for different sub-problems (like determining forces on the hydrofoils or the sail) and can be fed with data from experiments, CFD or even with approximations. In the following sections, we are primarily interested in the architecture of VPP, i. e. the way all modules work together in order to establish the equations for equilibrium and how they are subsequently solved. For this purpose, the modules will be filled only with approximations based on [5] and [6].

V. SAILOR POSITION MODULE

This module is the most mathematical one. It assumes a stick-man model for sailor's body and calculates position of his joints using methods of analytic geometry. During explaining the ideas behind VPP, we will introduce a few Cartesian coordinate systems (each module uses its own), but all with the same zero point. This module makes use of the board coordinate system (fig. 5) defined as follows. Its origin is situated on the top surface of the board at the position of the front screw of the foil mast. xy-plane coincides with the deck, with x-axis directed forward (from stern to bow) and y-axis directed windward. z-axis points upwards. In order to obtain right-handed system, we have to consider sailing on port.

Crucial elements of the geometry of windsurfing are the harness lines. For simplicity we assume the first configuration presented on figure 6, where points at which the lines are attached to the boom are close to each other. Also, we assume that the harness freely rotates around windsurfer's body and behaves like a ball joint. All mentioned simplifications reduce the somewhat complex constraints of the harness lines to a single condi-

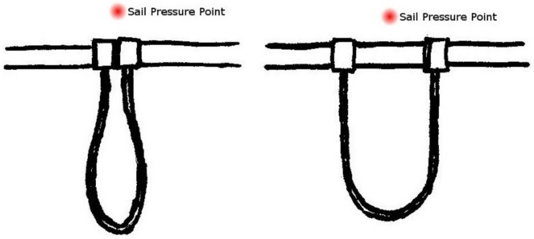

Figure 6: Two slightly different settings of the harness lines; picture taken from "How to windsurf 101" blog by Arne Gahmig, `https://howtowindsurf101.com/how-to-set-up-the-harness-lines/`

tion: Distance between point L (at which harness lines are attached to the boom) and some fixed point P on sailor's torso is constant and equal l_{eff} (fig. 7). We use a stick-man model for sailor's body, in which arms, legs and torso with head are straight lines. We have thus only two joints: K - connecting legs with torso and R - joining torso with arms. Point P in this approximation lies on the KR segment. We can introduce a unit vector $\hat{v}$ with direction along $\overrightarrow{KR}$ and two fixed distances x_1 and x_2, such that $P = K + x_1\hat{v}$ and $R = K + x_2\hat{v}$ (once we have set the origin of the coordinate system, each point X can be associated with a vector from that origin to X, so that we can perform operations on points as on vectors). Distance $|RL|$ is constrained by the length of arms, so we can write $|RL| = l_{\mathrm{arm}}$. Of course l_{arm} is only an effective length and it is shorter than arms if they are bent. We can perform similar reasoning for the legs. Let F_1 and F_2 be the position of the front and rear foot respectively. We assume F_1 to coincide with the front foot strap, but it is not the case for F_2 as the rear foot strap is often absent. We can write $|F_1K| = l_{\mathrm{eg1}}$, $|F_2K| = l_{\mathrm{eg2}}$, where l_{eg1} and l_{eg2} are effective lengths of the front and rear leg respectively (i. e. these distances are shorter when the legs are bent).

Summarizing, we end up with the following conditions:

$$\begin{aligned} |F_1K| &= l_{\mathrm{eg1}}, \quad |F_2K| = l_{\mathrm{eg2}}, \\ |RL| &= l_{\mathrm{arm}}, \quad\ |PL| = l_{\mathrm{eff}} \end{aligned} \tag{3}$$

With no additional conditions, there are five degrees of freedom in choosing position of point K and direction of vector $\hat{v}$. Four constraints from (3) leave us with just one remaining degree of freedom, which we call β. The task of the sailor position module is to find K and $\hat{v}$, given F_1, F_2, L and β (together with distances x_1, x_2, l_{eg1}, l_{eg2},l_{arm} and l_{eff}).

Let M be a projection of point K onto segment F_1F_2 (fig. 8). Let $h = |MK|$ and $d_f = |F_1F_2|$. We can introduce a parameter $u \in (0,1)$, such that $M = (1-u)\,F_1 + uF_2$. Thus $|F_1M| = d_f u$. Using Pythagorean Theorem, we have $h^2 = l_{\mathrm{eg1}}^2 - (d_f u)^2$ and $|MF_2| = \sqrt{l_{\mathrm{eg2}}^2 - h^2}$, so $|MF_2| = \sqrt{l_{\mathrm{eg2}}^2 - l_{\mathrm{eg1}}^2 + (d_f u)^2}$.

Figure 7: Distance $|PL| = l_{\mathrm{eff}}$; photo of Maciek Rutkowski provided by FotoSurf

Of course, $|F_1M| + |MF_2| = d_f$, which can be written now as:

$$d_f u + \sqrt{l_{\mathrm{eg2}}^2 - l_{\mathrm{eg1}}^2 + (d_f u)^2} = d_f \tag{4}$$

Solving for u, we get:

$$u = \frac{l_{\mathrm{eg1}}^2 - l_{\mathrm{eg2}}^2 + d_f^2}{2d_f^2} \tag{5}$$

Using

$$h = \sqrt{l_{\mathrm{eg1}}^2 - (d_f u)^2} = \sqrt{(l_{\mathrm{eg1}} - d_f u)\,(l_{\mathrm{eg1}} + d_f u)}$$

and substituting (5) for u, we get:

$$h = \frac{\sqrt{\left(l_{\mathrm{eg2}}^2 - (l_{\mathrm{eg1}} - d_f)^2\right)\left((l_{\mathrm{eg1}} + d_f)^2 - l_{\mathrm{eg2}}^2\right)}}{2d_f} \tag{6}$$

Position of K can be written as $M + \overrightarrow{h}$, where $\overrightarrow{h}$ is a vector of length h perpendicular to $\overrightarrow{F_2F_1}$. Direction of $\overrightarrow{h}$ has to be chosen so as to satisfy the second pair of constraints from (3). Let us write them using K and $\hat{v}$:

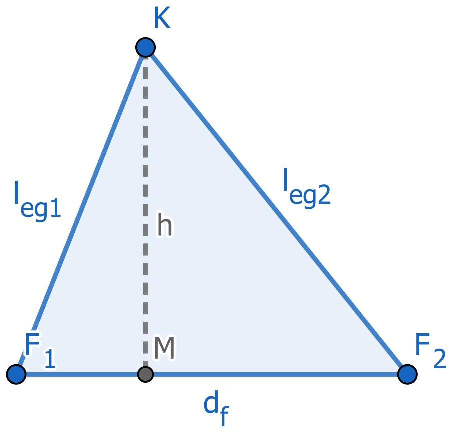

Figure 8: F_1F_2K triangle

$$\begin{cases} |K-L|^2 + x_1^2 + 2\,(K-L)\cdot\hat{v}x_1 = l_{\text{eff}}^2 \\ |K-L|^2 + x_2^2 + 2\,(K-L)\cdot\hat{v}x_2 = l_{\text{arm}}^2 \end{cases} \tag{7}$$

Rearranging terms in (7), we obtain:

$$\begin{cases} 2\,(K-L)\cdot\hat{v} = \frac{l_{\text{eff}}^2-\left(|K-L|^2+x_1^2\right)}{x_1} \\ 2\,(K-L)\cdot\hat{v} = \frac{l_{\text{arm}}^2-\left(|K-L|^2+x_2^2\right)}{x_2} \end{cases} \tag{8}$$

Thus:

$$\frac{l_{\text{eff}}^2 - \left(|K-L|^2 + x_1^2\right)}{x_1} = \frac{l_{\text{arm}}^2 - \left(|K-L|^2 + x_2^2\right)}{x_2} \tag{9}$$

Solving for $|K-L|^2$, we get:

$$|K-L|^2 = \left(\frac{l_{\text{eff}}^2 - x_1^2}{x_1} - \frac{l_{\text{arm}}^2 - x_2^2}{x_2}\right) / \left(\frac{1}{x_1} - \frac{1}{x_2}\right) \tag{10}$$

Using $|K-L|^2 = \left|M-L+\overrightarrow{h}\right|^2$, we can write:

$$|K-L|^2 = |M-L|^2 + h^2 + 2\,(M-L)\cdot\overrightarrow{h} \tag{11}$$

This gives:

$$(M-L)\cdot\hat{h} = \frac{|K-L|^2 - \left(|M-L|^2 + h^2\right)}{2h} \tag{12}$$

Equations (6) and (12), together with the fact $\overrightarrow{h}\perp\overrightarrow{F_2F_1}$ allow us to determine $\overrightarrow{h}$. We know the component of $\hat{h}$ along $M-L$, so it is useful to decompose it in the following way:

$$\hat{h} = \cos\vartheta\,\hat{p} + \sin\vartheta\,\hat{r}, \tag{13}$$

where $\overrightarrow{p} = (F_1 - F_2)\times(M-L)$, $\hat{p} = \overrightarrow{p}/|\overrightarrow{p}|$ and $\hat{r} = \hat{p}\times(F_1-F_2)$. Taking a scalar product of (13) with $M-L$ and exploiting the properties of a mixed product, we get:

$$\sin\vartheta = \frac{(M-L)\cdot\hat{h}}{(M-L)\cdot\hat{r}} \tag{14}$$

It is sufficient to put $\vartheta = \arcsin\left(\frac{(M-L)\cdot\hat{h}}{(M-L)\cdot\hat{r}}\right)$. There is another branch of the solution with negative sign of $\cos\vartheta$. This however corresponds to a situation, when $\hat{h}$ is directed downwards, which is not what occurs in practice.

Now we need to find $\hat{v}$ from (8). Special choice of $|K-L|^2$ (formula (10)), made the system of two equations for $\hat{v}$ indeterminate (in fact both became identical). Thus $\hat{v}$ can have any direction, provided that $(K-L)\cdot\hat{v}$ is as given by (8). This single degree of freedom can be parameterized by variable β as follows:

$$\hat{v} = \frac{K-L}{|K-L|^2}(K-L)\cdot\hat{v} + \left(\cos\beta\,\hat{a} + \sin\beta\,\hat{b}\right)\sqrt{1-\left(\frac{K-L}{|K-L|}\cdot\hat{v}\right)^2}, \tag{15}$$

where, for example, $\overrightarrow{a} = \hat{x}\times(K-L)$, $\hat{a} = \overrightarrow{a}/|\overrightarrow{a}|$ and $\hat{b} = \hat{a}\times\frac{K-L}{|K-L|}$. As β increases, sailor's torso shifts backwards. It is reasonable to assume $\beta\in[-\pi/2,\pi/2]$.

Closed-form formula for given geometrical problem could be built, nesting appropriate equations from above. This would yield very complex result, which is not in fact necessary, as obtained formulas are enough for constructing an algorithmic solution (fig. 9 shows an exemplary result).

VI. GLIDER MODULE

Glider module takes in just four state variables: speed v and three RPY angles θ_f, ϕ_f, ψ_f describing orientation of the board. It returns the total force and torque generated by the foils.

Let us introduce the "main" coordinate system. Its origin coincides with the board coordinate system. Its x-axis is directed as the velocity $\overrightarrow{v}$, y-axis is horizontal and directed windward, while z-axis is vertical (and directed upwards). Neutral orientation of the board (i. e. the one with $(\theta_f,\phi_f,\psi_f) = (0,0,0)$) corresponds to a situation when the board coordinate system coincides with the main coordinate system. In order to find the position of the board for $(\theta_f,\phi_f,\psi_f)\neq(0,0,0)$, we subsequently apply to it the following rotations. First we rotate it

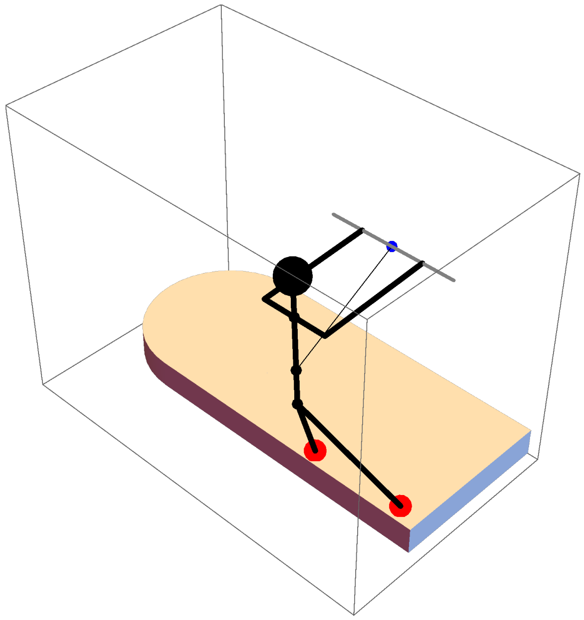

Figure 9: Stick-man model generated by the sailor position module

by angle ψ_f around the main z-axis. Secondly, we rotate it by angle $-\phi_f$ around the main y-axis and finally we rotate by $-\theta_f$ around the main x-axis. Presence of the minuses is to ensure that $\phi_f > 0$ means pitching up and $\theta_f > 0$ represents heeling to windward, as it usually occurs in the case of windsurfing foil.

Described transformation can be written as a 3D-rotation matrix given by equation (16).

Now we define the glider coordinate system, which we obtain by rotating all axes of the main coordinate system by angle $-\theta_f$ around the x-axis. Output of this module is given in this system, because it reduces the role of angle θ_f significantly. Neglecting water-air interface effects (i. e. waves), this output will be independent of θ_f, as all forces and torques are expected to simply rotate (together with the glider coordinate system) as θ_f is changed.

Inputs and outputs of the glider module are already defined. We are in a position to fill it with approximate formulas based on [5] and [6] as announced before. Among the RPY angles, θ_f takes the greatest values. Presence of some positive θ_f can be easily seen by eye, while visibility of $\phi_f > 0$ or $\psi_f > 0$ is rather subtle (take-off and very low speed are exceptions). For this reason, forces generated due to ϕ_f and ψ_f can be regarded as independent (in $\phi_f, \psi_f \ll 1$ approximation). ψ_f is just the angle of attack of the foil mast, so as long as we are away from stalling limit, lateral force is proportional to ψ_f. As for ϕ_f, it changes the angle of attack of the front wing, fuselage and the tail wing, so lift also increases with it linearly. Zero-lift angle can differ significantly from $\phi_f = 0$, due to the rake and the glider itself. Thus lift can be said to be proportional to $\phi_f - r$, where r is some effective rake angle. To complete the model, drag can be expressed as a quadratic function of lift and appropriate factors have to be included. The total force $\overrightarrow{F}_f$, generated by the foils, has the following components in the glider coordinate system (equation (17)):

$$\overrightarrow{F}_f = \frac{1}{2}\rho_w v^2 S_1 \begin{bmatrix} -C_D \\ C_{Lm} \\ C_{Lf} \end{bmatrix}_{\text{glider}}, \tag{17}$$

with

$$\begin{cases} C_{Lm} = \frac{S_m}{S_1} s_m \psi_m \\ C_{Lf} = s_f\,(\phi_f - r) \\ C_D = \mathcal{A}_f C_{Lf}^2 + \mathcal{B}_f C_{Lf} + \mathcal{C}_f \\ +\mathcal{A}_m C_{Lm}^2 + \mathcal{B}_m C_{Lm} + \mathcal{C}_m \end{cases} \tag{18}$$

ρ_w is the water density. S_1 is the planform area of the front wing. S_m is the wetted area of the foil mast and s_m is its lift-curve slope. s_f is the effective lift-curve slope for the glider (for vertical lift). Coefficients $\mathcal{A}_f, \mathcal{B}_f, \mathcal{C}_f, \mathcal{A}_m, \mathcal{B}_m, \mathcal{C}_m$ are present just to approximate drag as a quadratic function of lift. Values of $\mathcal{A}_m, \mathcal{B}_m, \mathcal{C}_m$ depend on the depth of submersion, due to changes in the aspect ratio of the mast wetted part.

In the case of torque, we have:

$$\overrightarrow{\tau}_f = \frac{1}{2}\rho_w v^2 S_1 \times \begin{bmatrix} (t_{\text{board}} + H - \kappa h_m)\, C_{Lm} \\ \begin{pmatrix} -l_{AC} C_{Lf} - l C_{\tau f} + (t_{\text{board}} + H)\, C_{Df} \\ +\,(t_{\text{board}} + H - \kappa h_m)\, C_{Dm} \end{pmatrix} \\ 0 \end{bmatrix}_{\text{glider}} \tag{19}$$

t_{board} is the thickness of the board (on the stern). H is the total height of the foil mast, while h_m is its wetted part. κ is a factor indicating the vertical position of the hydrodynamic center of the foil mast. l_{AC} is the position of the neutral point of the glider. l is the length of the fuselage. $C_{\tau f}$ is the pitching moment coefficient of the glider referred to l. $C_{Df} = \mathcal{A}_f C_{Lf}^2 + \mathcal{B}_f C_{Lf} + \mathcal{C}_f$ and $C_{Dm} = \mathcal{A}_m C_{Lm}^2 + \mathcal{B}_m C_{Lm} + \mathcal{C}_m$. Vanishing of the z-component of $\overrightarrow{\tau}$ is due to the choice of the point of reference (which is the common origin of the coordinate systems): Front screw of the foil mast is roughly above its hydrodynamic center. Even if it is not so, we can shift the reference point to satisfy this condition (after all position of the screw itself does not affect performance).

VII. SAIL MODULE

This module is designed in full analogy to the glider module. The only difference is that the velocity $\overrightarrow{v}$ gets

$$T_{\mathrm{RPY}}(\theta,\phi,\psi)=\begin{pmatrix}\cos\psi\cos\phi & -\sin\psi\cos\phi & -\sin\phi\\ \cos\theta\sin\psi+\sin\theta\cos\psi\sin\phi & \cos\theta\cos\psi-\sin\theta\sin\psi\sin\phi & \sin\theta\cos\phi\\ \cos\theta\cos\psi\sin\phi-\sin\theta\sin\psi & -\sin\theta\cos\psi-\cos\theta\sin\psi\sin\phi & \cos\theta\cos\phi\end{pmatrix} \tag{16}$$

replaced by the apparent wind velocity with reversed direction $-\overrightarrow{v}_A$. Orientation of the sail (or actually the entire rig) is given by three RPY angles θ_s, ϕ_s, ψ_s. Neutral position can be chosen arbitrarily, but it seems most natural to set it at zero angle of attack and no sweep. Sail coordinate system is obtained as follows. x-axis is directed as vector $-\overrightarrow{v}_A$. For $\theta_s = 0$, y-axis is horizontal and directed windward (when referred to the true wind) and z-axis is vertical (pointing upwards). If $\theta_s \neq 0$, these axes have to be rotated by $-\theta_s$ around the x-axis.

Significant twist and variable camber along the span characterize windsurfing sails. This makes the airflow past them rather complicated. Given sail has basically two changeable parameters: downhaul and outhaul regulation. The first changes tension on the mast and thus its curvature, which affects twist and shape in general (also camber). It is an equipment parameter. The second influences mainly camber and can be varied during sailing. Thus it is described by an additional state parameter, which we denote by ψ_0. Sail works usually with some nonzero sweep. This actually makes only CFD (or experimental) data reliable. Nevertheless, for now, we want some toy model to fill this module and obtain at least qualitative predictions. Problem of sweep can be handled by invoking the cross-flow principle (from [5] and [6]), which states that the component of the free stream velocity parallel to the span-wise direction can be neglected. This reduces the flow to the no sweep situation. Lift coefficient C_{Ls} can be approximated by a linear function of ψ_s and drag coefficient C_{Ds} by a quadratic function of C_{Ls}. Zero-lift angle depends on the camber, so we can assign value of this angle to ψ_0. This gives:

$$\overrightarrow{F}_s = \frac{1}{2}\rho_a v_A^2 \cos^2\phi_s S_s \left(T_{\mathrm{RPY}}(0,\phi_s,0)\begin{bmatrix}-C_{Ds}\\ -C_{Ls}\\ 0\end{bmatrix}\right)_{\mathrm{sail}}, \tag{20}$$

with

$$\begin{cases} C_{Ls} = s_s(-\psi_s+\psi_0)\\ C_{Ds} = \mathcal{A}_s C_{Ls}^2 + \mathcal{B}_s C_{Ls} + \mathcal{C}_s \end{cases} \tag{21}$$

Subscript sail indicates that the components are given in the sail coordinate system. ρ_a is the air density. S_s is the sail area and s_s is the lift-curve slope. Coefficients $\mathcal{A}_s$, $\mathcal{B}_s$, $\mathcal{C}_s$ play analogous role to $\mathcal{A}_f$, $\mathcal{B}_f$, $\mathcal{C}_f$ and $\mathcal{A}_m$, $\mathcal{B}_m$, $\mathcal{C}_m$. Presence of $\cos\phi_s$ and $T_{\mathrm{RPY}}(0,\phi_s,0)$ is due to the cross-flow principle. If $s_s(-\psi_s+\psi_0)$ exceeds the maximal lift coefficient $C_{Ls\mathrm{Max}}$, we are unarguably out of the range of applicability of the linear approximation. It starts to be not accurate already for smaller values of C_{Ls}, but here is the limit when it gives opposite trend (further increasing of the angle of attack decreases lift). This problem can be avoided as follows (keeping in mind that it is only a toy model): If $s_s(-\psi_s+\psi_0) > C_{Ls\mathrm{Max}}$, we follow (21) normally, but then reduce C_{Ls} down to $C_{Ls\mathrm{Max}}$ (in other words we evaluate C_{Ds} with the overestimated value of C_{Ls}). This leads to further increasing drag C_{Ds} for $s_s(-\psi_s+\psi_0) > C_{Ls\mathrm{Max}}$ with no increment in C_{Ls}. Thus situation $s_s(-\psi_s+\psi_0) = C_{Ls\mathrm{Max}}$ is always more favorable than $s_s(-\psi_s+\psi_0) > C_{Ls\mathrm{Max}}$, which imitates stalling.

Total torque on the sail (exerted by aerodynamic forces) is calculated with respect to the mast foot. It can be approximated as follows:

$$\begin{aligned}\overrightarrow{\tau}_s &= \left(T_{\mathrm{RPY}}(0,\phi_s,\psi_s)\,\mathbf{r}_{AC}\right)_{\mathrm{sail}} \times \overrightarrow{F}_s\\ &+ \frac{1}{2}\rho_a v_A^2\cos^2\phi_s S_s c_s C_{\tau s}\left(T_{\mathrm{RPY}}(0,\phi_s,0)\begin{bmatrix}0\\0\\1\end{bmatrix}\right)_{\mathrm{sail}}\end{aligned} \tag{22}$$

$\mathbf{r}_{AC}$ is a column matrix (a vector) representing the components of the position vector (relative to the mast foot) of the sail aerodynamic center in the neutral orientation. It is regarded as a constant here, which in general should depend on ψ_0. $C_{\tau s}$ is the pitching moment coefficient referring to the cord length c_s.

VIII. BOARD MODULE

A windsurfing foil racing board has a considerable size when compared to other water sports employing a board. This is mainly due to the need of exerting sufficient righting moment to the set. Moreover, the board is rigidly connected to the foils, so its angle of attack cannot be prevented from changing. Thus aerodynamic forces generated on it should be taken into account.

It is convenient to follow the same convention as for the sail. We use three RPY angles θ_b, ϕ_b, ψ_b describing orientation of the board relative to its neutral one (which occurs when the x-axis of the board coordinate system is parallel to $-\overrightarrow{v}_A$, y-axis is horizontal and directed windward, while z-axis is vertical and directed upwards). If we take the axes of the board coordinate system at its neutral orientation and than rotate them by $-\theta_b$ around the x-axis, we obtain the "output board coordinate system", in which the output of this module is given. This is exactly the same idea, which we used for the sail, but now the term "board coordinate system" is reserved for that rigidly fixed to the board itself. Now the glider, sail and board modules are compatible in the way they take inputs and return outputs relative to the flow of the corresponding fluids.

The problem is, that θ_b, ϕ_b, ψ_b are not state variables, but rather they can be expressed in terms of them. This issue arises from the fact that the glider and the board are rigidly connected, while immersed in two different fluids, which free-stream velocities are not parallel. Let $\hat{x}_b, \hat{y}_b$ and $\hat{z}_b$ denote unit vectors with directions along axes of the board coordinate system. Let $\hat{v}_A = \overrightarrow{v}_A / v_A$. The following simple dot products can be used to calculate θ_b, ϕ_b, ψ_b:

$$\hat{z}_b \cdot \hat{v}_A = \sin \phi_b \tag{23}$$

$$\hat{y}_b \cdot \hat{v}_A = \sin \psi_b \cos \phi_b \tag{24}$$

$$(\hat{x}_b \sin \psi_b + \hat{y}_b \cos \psi_b) \cdot \hat{z} = -\sin \theta_b \tag{25}$$

$\hat{z}$ is a unit vector directed vertically (i. e. along z-axis of the main coordinate system). Thus:

$$\phi_b = \arcsin\left(\hat{z}_b \cdot \hat{v}_A\right) \tag{26}$$

$$\psi_b = \arcsin\left(\frac{\hat{y}_b \cdot \hat{v}_A}{\cos \phi_b}\right) \tag{27}$$

$$\theta_b = -\arcsin\left((\hat{x}_b \sin \psi_b + \hat{y}_b \cos \psi_b) \cdot \hat{z}\right) \tag{28}$$

In order to express θ_b, ϕ_b, ψ_b in terms of θ_f, ϕ_f, ψ_f and α, we can write unit vectors in formulas (26)-(28) in the main coordinate system:

$$\hat{x}_b = \left(T_{\text{RPY}}\left(\theta_f, \phi_f, \psi_f\right) \begin{bmatrix} 1 \\ 0 \\ 0 \end{bmatrix}\right)_{\text{main}} \tag{29}$$

$$\hat{y}_b = \left(T_{\text{RPY}}\left(\theta_f, \phi_f, \psi_f\right) \begin{bmatrix} 0 \\ 1 \\ 0 \end{bmatrix}\right)_{\text{main}} \tag{30}$$

$$\hat{z}_b = \left(T_{\text{RPY}}\left(\theta_f, \phi_f, \psi_f\right) \begin{bmatrix} 0 \\ 0 \\ 1 \end{bmatrix}\right)_{\text{main}} \tag{31}$$

$$\hat{v}_A = \left(T_{\text{RPY}}\left(0, 0, \alpha\right) \begin{bmatrix} -1 \\ 0 \\ 0 \end{bmatrix}\right)_{\text{main}} \tag{32}$$

It is useful to find the unit vectors $\hat{x}_{ob}$, $\hat{y}_{ob}$, $\hat{z}_{ob}$ corresponding to the axes of the output board coordinate system:

$$\hat{x}_{ob} = -\hat{v}_A,\ \hat{y}_{ob} = \frac{\hat{v}_A \times \hat{z}_b}{|\hat{v}_A \times \hat{z}_b|},\ \hat{z}_{ob} = -\hat{v}_A \times \hat{y}_{ob} \tag{33}$$

No "filling" of this module will be proposed, because the VPP can be launched without it (which is not true in the case of the glider or sail modules).

IX. SAILOR WINDAGE MODULE

Sailor's body creates aerodynamic drag D_W. For present purposes it is assumed to be independent of sailor's position, so we need just one parameter to describe it, namely the effective drag area S_W. Then:

$$D_W = \frac{1}{2} \rho_a v_A^2 S_W \tag{34}$$

This force can be assumed to act on some point of the form $K + x_w \hat{v}$.

X. CENTER OF MASS MODULE

For given RPY angles $\theta_f, \phi_f, \psi_f, \theta_s, \phi_s, \psi_s$, point K and unit vector $\hat{v}$, geometry of flight is fully determined. Knowledge of masses of each component allows us to calculate the total mass M and its center C_M. The same is done for the sailor alone, based on his stick-man model and statistical data from [7].

XI. COMBINING OUTPUTS OF THE MODULES

Now we are in a position to determine the ten equations indicating equilibrium of the foil in a flight by combining outputs of the mentioned modules. Let us write all ten basic state variables:

$$v, \theta_s, \phi_s, \psi_s, \theta_f, \phi_f, \psi_f, \beta, T_{\text{lines}}, \tau_{\text{arms}} \tag{35}$$

together with the additional state variables:

$$\psi_0, F_{2x}, F_{2y}, l_{\text{eg1}}, l_{\text{eg2}} \tag{36}$$

F_{2x}, F_{2y} are coordinates (in the board coordinate system) of the point F_2. T_{lines} refers to the tension of the harness lines and τ_{arms} is the torque applied to the boom by sailor's arms. We will express all further formulas in terms of the input variables v_T, φ and those from (35) and (36).

Apparent wind speed v_A and angle α can be calculated using the wind diagram (fig. 1), the cosine and sine laws:

$$v_A = \sqrt{v_T^2 + v^2 + 2v_T v \cos\varphi} \quad (37)$$

$$\alpha = \arcsin\left(\frac{v_T}{v_A}\sin\varphi\right) \quad (38)$$

First, we calculate the net force acting on the entire system. We write it in a form, such that it is straightforward to obtain its components in the main coordinate system.

$$\vec{F}_{\text{net}} = \begin{bmatrix} 0 \\ 0 \\ -Mg \end{bmatrix}_{\text{main}} + \underbrace{\left(T_{\text{RPY}}(\theta_f, 0, 0)\,\mathbf{F}_f\right)_{\text{main}}}_{\vec{F}_f} + \underbrace{\left(T_{\text{RPY}}(0,0,\alpha)\,T_{\text{RPY}}(\theta_s,0,0)\,\mathbf{F}_s\right)_{\text{main}}}_{\vec{F}_s} + \underbrace{[\hat{x}_{ob}, \hat{y}_{ob}, \hat{z}_{ob}]\,\mathbf{F}_b}_{\vec{F}_b} + D_W \hat{v}_A, \quad (39)$$

g is the acceleration due to gravity. $\mathbf{F}_f$, $\mathbf{F}_s$ and $\mathbf{F}_b$ represent force components returned by the glider, sail and board modules respectively. $\vec{F}_b$ is the total force acting on the board (as a vector in absolute notation).

Secondly, we do the same thing for the net torque. Sailor's position is meaningful here, but the module responsible for that needs coordinates of the point L in the board coordinate system. L is fixed to the rig, so its coordinates $\mathbf{L}_0$ in the sail coordinate system at $(\theta_s, \phi_s, \psi_s) = (0, 0, 0)$ should be regarded as equipment parameters. We can calculate coordinates of L in the board coordinate system (denoted as $\mathbf{L}_b$) by applying the following rotations and translations:

$$\mathbf{L}_b = \mathbf{R}\left(\mathbf{L}_0 - \begin{bmatrix} x_{\text{foot}} \\ 0 \\ 0 \end{bmatrix}\right) + \begin{bmatrix} x_{\text{foot}} \\ 0 \\ 0 \end{bmatrix}, \quad (40)$$

where

$$\mathbf{R} = \left(T_{\text{RPY}}(\theta_f, \phi_f, \psi_f)\right)^{-1} T_{\text{RPY}}(0,0,\alpha)\,T_{\text{RPY}}(\theta_s, \phi_s, \psi_s)$$

x_{foot} is the distance from the common origin of coordinate systems and the mast foot. Subtracting $[x_{\text{foot}}, 0, 0]^T$ from $\mathbf{L}$ is equivalent to shifting the origin to the mast foot. Strictly speaking, it is the position of the rubber joint that is relevant, so $[x_{\text{foot}}, 0, 0]^T$ should, in general, contain some small nonzero z-component. Formula (40) follows simply from the fact, that both

$$T_{\text{RPY}}(0,0,\alpha)\,T_{\text{RPY}}(\theta_s, \phi_s, \psi_s)\left(\mathbf{L}_0 - \begin{bmatrix} x_{\text{foot}} \\ 0 \\ 0 \end{bmatrix}\right)$$

and

$$T_{\text{RPY}}(\theta_f, \phi_f, \psi_f)\left(\mathbf{L}_b - \begin{bmatrix} x_{\text{foot}} \\ 0 \\ 0 \end{bmatrix}\right)$$

are equal and represent the coordinates of L in the main coordinate system (shifted so that the origin is at the mast foot).

The net torque $\vec{\tau}_{\text{net}}$ (measured with respect to the common origin of the coordinate systems) can be now calculated:

$$\vec{\tau}_{\text{net}} = \left(\mathbf{C}_M \times \begin{bmatrix} 0 \\ 0 \\ -Mg \end{bmatrix}\right)_{\text{main}} + \underbrace{\left(T_{\text{RPY}}(\theta_f, 0, 0)\,\boldsymbol{\tau}_f\right)_{\text{main}}}_{\vec{\tau}_f} + \underbrace{\left(T_{\text{RPY}}(0,0,\alpha)\,T_{\text{RPY}}(\theta_s,0,0)\,\boldsymbol{\tau}_s\right)_{\text{main}}}_{\vec{\tau}_s} + \left(T_{\text{RPY}}(\theta_f, \phi_f, \psi_f)\begin{bmatrix} x_{\text{foot}} \\ 0 \\ 0 \end{bmatrix}\right)_{\text{main}} \times \vec{F}_s + \underbrace{[\hat{x}_{ob}, \hat{y}_{ob}, \hat{z}_{ob}]\,\boldsymbol{\tau}_b}_{\vec{\tau}_b} + \underbrace{\left(T_{\text{RPY}}(\theta_f, \phi_f, \psi_f)\,(\mathbf{K} + x_w \hat{\mathbf{v}})\right)_{\text{main}}}_{K + x_w \hat{v}} \times (D_W \hat{v}_A) \quad (41)$$

$\mathbf{C}_M$ is the output of the center of mass module. $\boldsymbol{\tau}_f$, $\boldsymbol{\tau}_s$ and $\boldsymbol{\tau}_b$ represent torque components returned by the glider, sail and board modules respectively. $\mathbf{K}$ and $\hat{\mathbf{v}}$ are components of the K and $\hat{v}$ vectors in the board coordinate system (they are returned by the sailor position module). Torque due to the board and the glider is given with respect to the common origin. In the case of the sail, $\vec{\tau}_s$ is measured with respect to the mast foot, which results in an additional term (fourth line in (41)).

We have already established six equations governing the performance of the foil, which can be written as $\vec{F}_{\text{net}} = 0$, $\vec{\tau}_{\text{net}} = 0$. There are yet four equations left, corresponding to the net torque on the sail $\vec{\tau}_{\text{sail}}$ (measured with respect to the mast foot) and one component of the torque on the sailor τ_{sailor}. The latter is measured with respect to the the front foot F_1 along direction F_1F_2. In order to calculate these quantities we need to specify precisely the meaning of τ_{arms}. We assume that the total force exerted on the boom by arms is zero, in other words, left and right arms act with opposite forces, which results only in some torque. This minimizes the loads on arms and even though different distributions of forces are possible, they are not considered maintainable for longer time and are excluded from further analysis. Forces due to the arms are assumed to be parallel to

$K + x_2\hat{v} - L$. Let $\overrightarrow{r}_{\text{hands}}$ denote a vector from the rear hand to the front one. Torque τ_{arms} has direction along the vector $-\overrightarrow{r}_{\text{hands}} \times (K + x_2\hat{v} - L)$. In this sign convention, $\tau_{\text{arms}} > 0$ corresponds to pulling the rear arm. $\overrightarrow{r}_{\text{hands}}$ is roughly parallel to the tangent to the boom at point L. If $\mathbf{r}_{\text{hands}}$ denotes the components of $\overrightarrow{r}_{\text{hands}}$ in the sail coordinate system at $(\theta_s, \phi_s, \psi_s) = (0, 0, 0)$, it can be regarded as equipment parameter. Then direction of τ_{arms} can be calculated as direction of the following vector given in the main coordinate system:

$$\begin{aligned}\mathbf{D} = &-\left(T_{\text{RPY}}\left(0,0,\alpha\right) T_{\text{RPY}}\left(\theta_s,\phi_s,\psi_s\right)\mathbf{r}_{\text{hands}}\right) \\ &\times \left(T_{\text{RPY}}\left(\theta_f,\phi_f,\psi_f\right)\left(\mathbf{K} + x_2\hat{\mathbf{v}} - \mathbf{L}_b\right)\right) \quad (42)\end{aligned}$$

Now $\overrightarrow{\tau}_{\text{sail}}$ and τ_{sailor} can be written out:

$$\begin{aligned}&\overrightarrow{\tau}_{\text{sail}} = \overrightarrow{\tau}_s \\ &+ \left(T_{\text{RPY}}\left(0,0,\alpha\right) T_{\text{RPY}}\left(\theta_s,\phi_s,\psi_s\right)\mathbf{C}_{m\text{sail}}\right)_{\text{main}} \times \begin{bmatrix} 0 \\ 0 \\ -m_{\text{sail}}g \end{bmatrix}_{\text{main}} \\ &+ \left(T_{\text{RPY}}\left(\theta_f,\phi_f,\psi_f\right)\left(\mathbf{L}_b - \begin{bmatrix} x_{\text{foot}} \\ 0 \\ 0 \end{bmatrix}\right)\right)_{\text{main}} \times T_{\text{lines}}\hat{T}_{\text{lines}} \\ &+\tau_{\text{arms}}\left(\frac{\mathbf{D}}{|\mathbf{D}|}\right)_{\text{main}} \quad (43)\end{aligned}$$

m_{sail} is the mass of the rig. $\mathbf{C}_{m\text{sail}} + [x_{\text{foot}}, 0, 0]^T$ is the position of the center of mass of the rig at $(\theta_s, \phi_s, \psi_s) = (0, 0, 0)$ in the main coordinate system. $\hat{T}_{\text{lines}}$ is a unit vector obtained by normalizing $\left(T_{\text{RPY}}\left(\theta_f,\phi_f,\psi_f\right)\left(\mathbf{K} + x_1\hat{\mathbf{v}} - \mathbf{L}_b\right)\right)_{\text{main}}$.

$$\begin{aligned}&\tau_{\text{sailor}} = \\ &\Bigg(\left(T_{\text{RPY}}\left(\theta_f,\phi_f,\psi_f\right)\left(\mathbf{C}_{m\text{sailor}} - \mathbf{F}_1\right)\right)_{\text{main}} \times \begin{bmatrix} 0 \\ 0 \\ -m_{\text{sailor}}g \end{bmatrix}_{\text{main}} \\ &- \left(T_{\text{RPY}}\left(\theta_f,\phi_f,\psi_f\right)\left(\mathbf{K} + x_1\hat{\mathbf{v}} - \mathbf{F}_1\right)\right)_{\text{main}} \times T_{\text{lines}}\hat{T}_{\text{lines}} \\ &-\tau_{\text{arms}}\left(\frac{\mathbf{D}}{|\mathbf{D}|}\right)_{\text{main}}\Bigg) \cdot \frac{\overrightarrow{F_2F_1}}{|F_2F_1|} \quad (44)\end{aligned}$$

$\mathbf{C}_{m\text{sailor}}$ is the position of the center of mass of the sailor in the board coordinate system. $\mathbf{F}_1$ and $\mathbf{F}_2$ represent the coordinates of points F_1 and F_2 respectively (in the board coordinate system). m_{sailor} is sailor's mass. Vector $\overrightarrow{F_2F_1}$ can be expressed as $\left(T_{\text{RPY}}\left(\theta_f,\phi_f,\psi_f\right)\left(\mathbf{F}_1 - \mathbf{F}_2\right)\right)_{\text{main}}$.

We have presented how to combine outputs of the modules, in order to calculate $\overrightarrow{F}_{\text{net}}$, $\overrightarrow{\tau}_{\text{net}}$, $\overrightarrow{\tau}_{\text{sail}}$ and τ_{sailor}, which equated to 0 give the ten equations governing the performance of the foil. In subsequent sections, we turn to the problem of solving them numerically.

XII. DIFFICULTIES IN FINDING A SOLUTION

Complexity of the equations which we want to solve, gives us no clue about the number or even existence of the roots. However, we know that there are "physical" solutions, because the equations represent a situation well-known from practice - steady sailing on course. VPPs usually employ the Newton-Raphson algorithm for solving non-linear systems of equations (because of its speed). It has two important disadvantages though: Jacobian has to be calculated and good starting point is required. We cannot easily determine the derivatives of the established equations, but finite differences can be used instead. The latter issue is slightly more problematic. Choosing a random starting point usually does not provide convergence. It is not a problem in general, because if at least one solution for given parameters (i. e. input variables, additional variables and equipment parameters) is known, we can change them in small steps, each time solving the equations with the starting point taken from the last step. If the changes are sufficiently small in each update, convergence is provided. Finally a solution for arbitrary parameters can be found. This method (similar in its spirit to homotopy [8]) cannot be used to find the solution for the first time. Two different approaches have been used for this task.

The first is a brute force method, in which we pick a random starting point (chosen from the physically possible subset of the state space), then we run the Newton-Raphson. The procedure is repeated until convergence is obtained. Even though such algorithm is very inefficient, it is acceptable, as we use it only once (before any solutions are known). It is good to mention that running it many times gave exactly two distinct roots. The way hydrodynamic drag is modeled in the glider module is responsible for that. When $v \to 0^+$, profile drag of the horizontal foils tends to zero, but for given constant lift, induced drag tends to infinity. When $v \to \infty$, the situation is reversed, profile drag tends to infinity, but induced drag (for given lift) tends to zero. Thus the same hydrodynamic drag may be achieved at two different speeds. This may lead to existence of two different solutions. That with lower value of v is often unstable, because when the induced drag dominates, increasing speed reduces drag. Even if it is not the case, the solution with greater value of v should be always considered, as it is preferable.

The second approach is more sophisticated and exploits some physical intuitions. It is explained in the next section.

XIII. EQUATION BY EQUATION METHOD

This strategy is based on qualitative knowledge of the forces and torques involved (fig. 4). Sailing is possible primarily due to the presence of the sail thrust (arrow number 1). It is opposed by the hydrodynamic drag (arrow number 6), which results in some finite equilibrium speed. Of course, it is not the full story. This corresponds just to one equation $F_x = 0$ (where F_x denotes the x-component of $\overrightarrow{F}_{\text{net}}$ in the main coordinate system). Final speed is influenced by other equations as well, for example heavy sailor will need slightly more pitch angle in order to satisfy $F_z = 0$, which leads to greater induced drag on the front wing. Even though influence of these equations on speed is high, we can obtain the first (very rough) approximation by solving $F_x = 0$ alone for v, treating other basic state variables as constant.

When θ_s, ϕ_s, ψ_s are held constant and v changes, apparent wind angle α varies and thus the orientation of the sail too. If RPY angles θ_s, ϕ_s, ψ_s and θ_f, ϕ_f, ψ_f have certain values, sailor position module returns complex numbers, because its geometrical task is unsolvable. For this reason, F_x as a function of v alone can be complex for some inputs and real-valued elsewhere. This complicates solving $F_x = 0$. In order to avoid the problem, we can replace θ_s, ϕ_s, ψ_s (which refer to the apparent wind angle $-\overrightarrow{v}_A$) by $\theta'_s, \phi'_s, \psi'_s$ (referring to $\overrightarrow{v}$ similarly as the RPY angles θ_f, ϕ_f, ψ_f of the glider), for the role of basic state variables. Given $(\theta'_s, \phi'_s, \psi'_s)$, we can calculate $(\theta_s, \phi_s, \psi_s)$ (which is necessary to use the sail module) in the same way, as given $(\theta_f, \phi_f, \psi_f)$, we calculate $(\theta_b, \phi_b, \psi_b)$ (formulas (26)-(28)). Now F_x as a function of v behaves much more intuitively. Increasing v decreases α and magnifies profile drag of the foils. Even though induced drag decreases, this is a minor effect for operational speeds, so generally $\partial F_x/\partial v < 0$. This condition provides a stable solution. Solving $F_x = 0$ can be done in almost no time by the Newton-Raphson algorithm. Starting value of v should be taken sufficiently large, to find the stable solution. There may exist an unstable one for unusually low speeds (as explained before).

We can make the next step towards solving the full system by considering three equations at once. In order to satisfy $F_y = 0$ and $F_z = 0$, lift generated on the foils (arrows 4 and 5) is needed. It is produced by appropriate angles of attack $\phi_f - r$ and ψ_f. Their values influence total hydrodynamic drag (arrow 6) and thus speed too. Now we consider system $\overrightarrow{F}_{\text{net}} = 0$ for variables v, ϕ_f, ψ_f. Starting point is chosen from the previous result. Remaining basic state variables are regarded still as constants.

We keep adding equations and state variables until we solve the entire system. The general idea is to choose pairs equation-variable so that the former strongly depends on the latter (so that the newly added equation can be satisfied by adjusting the value of the newly added variable). It is perfect when other equations are weakly dependent on this variable, because values of already included variables would not change significantly after next update. Of course, this is not always possible.

In the spirit of the mentioned rule, we seek for an equation, which can be paired with θ_f. Due to some nonzero heel, not only the foil mast takes part in generating the hydrodynamic lateral (horizontal) force, but also the main foil. Total magnitude of this force is determined by the aerodynamic side force and depending on the heel, it is split among the vertical and horizontal foils. Center of pressure of the front and tail wings (considered together) is well ahead of that of the foil mast. Thus distributing more of the lateral force on the main foil (which occurs for greater θ_f), brings some yawing torque, which increases τ_z (z component of $\overrightarrow{\tau}_{\text{net}}$ in the main coordinate system). It is reasonable then to pair equation $\tau_z = 0$ with variable θ_f. To justify it even more simply, we can note that turning on the foil is realized by heeling the board.

Remaining components of the net torque: τ_x and τ_y can be paired with θ'_s and β. Justification is as follows. Windsurfers lean back (increasing θ'_s) until $\tau_x = 0$ is satisfied. In the learning process it sometimes happens, that θ'_s is insufficient, so $\tau_x > 0$ and the sailor gets drawn by the rig to the leeward side. If the lean is exaggerated (too large θ'_s), $\tau_x < 0$ and the windsurfer falls back into the water (on the windward side). Increasing β shifts sailor's mass backwards, which diminishes τ_y.

Equation $\tau_{\text{sailor}} = 0$ can be paired with variable T_{lines}, since the lines hold the windsurfer in a position. Torque τ_{arms} is applied to the sail and is roughly directed upwards, so this variable can be paired with equation $\tau_{\text{sail}z} = 0$.

Last two variables ϕ'_s and ψ'_s correspond clearly to $\tau_{\text{sail}y}$ and $\tau_{\text{sail}x}$ respectively. When the sail pitches up (ϕ'_s increases), its center of mass shifts backwards, which decreases $\tau_{\text{sail}y}$. Smaller ψ'_s magnifies tension on the sail and thus increases $\tau_{\text{sail}x}$.

Finally, we get the following order of pairs equation-variable:

$$\begin{array}{cccccccccc} v, & \phi_f, & \psi_f, & \theta_f, & \theta'_s, & \beta, & T_{\text{lines}}, & \tau_{\text{arms}}, & \phi'_s, & \psi'_s \\ F_x, & F_z, & F_y, & \tau_z, & \tau_x, & \tau_y, & \tau_{\text{sailor}}, & \tau_{\text{sail}z}, & \tau_{\text{sail}y}, & \tau_{\text{sail}x} \end{array} \tag{45}$$

Of course, it could have been done in many different ways. Described method is a way of finding a certain path towards the final solution in steps, so that Newton-Raphson can converge each time. It does not guarantee success, which is partly dependent on the choice of the starting point (or more precisely the values of the state variables that are held initially constant). Anyway, it is based on some intuitions, which are worth mentioning. It is also faster than the brute force approach. Equation by equation method solved the system in 0.8 second (for certain values of the parameters), while the average time of the random search was 2.4 seconds.

XIV. GENERATING A POLAR PLOT

Generating a polar plot for given v_T can be sensibly performed by means of the step-by-step method similar to homotopy. We want to solve the equations for a range of true wind angles φ. After obtaining the first solution (for example using the random search), we update φ by a small increment $\Delta\varphi$. Using the last result as the starting point for the current solving guarantees that we are close to the root. This increases chances of convergence. If it turns out not to be close enough, $\Delta\varphi$ can be reduced. This process is repeated until we cover the relevant interval of φ values. Figure 10a shows the result of such process for $v_T = 6\,\frac{\mathrm{m}}{\mathrm{s}}$. Obtained shape possesses a few unexpected features. First of all, upwind speed is greater than downwind speed. Secondly, the curve representing speed changes sign of curvature. These properties are possible, but they are very atypical for sailing hydrofoils.

The reason of these anomalies becomes clear, when we think about the additional state variables. They were held constant during solving. However, this is not exactly what happens with them in practice. Sailor changes them so as to maximize speed. Now, instead of just solving nonlinear equations, optimization is necessary.

XV. OPTIMIZING ADDITIONAL STATE VARIABLES

Solving the ten equations with different additional state variables, gives in general different speed v in the solution. Thus we are faced with some function (returning v, with the additional state variables as arguments), which we want to maximize. This approach treats the basic and additional state variables on unequal footing. Actually, they play exactly the same role. We are given n equations for speed v and m different variables. In our model, $n = 10$ and $m = 14$ (it is the total number of the basic and additional state variables together without counting v). $m > n$, so for fixed v we have an underdetermined system. Let $v_{\max}$ denote the maximal speed. Considered system of equations has no roots for $v > v_{\max}$, while for $v < v_{\max}$ we expect infinitely many solutions. v is now not an unknown, but a parameter. Having a solution for certain speed $v_0 < v_{\max}$, we can easily search for a root (one out of infinitely many) for some speed $v_0 + \Delta v < v_{\max}$, in the same way, as we did it varying φ. The only difference is that we deal with an underdetermined system, so an inverse of the Jacobi matrix in the Newton-Raphson algorithm must be replaced by the Moore-Penrose pseudoinverse [9, 10]. If finally a root is not found, there are two possibilities. Δv is too large or $v_0 + \Delta v$ exceeded $v_{\max}$. If we keep reducing Δv sufficiently, the first possibility is excepted. This method allows to determine $v_{\max}$ with maximal uncertainty of Δv.

Applying described optimization method to the polar plot generated before, we get the result presented in figure 10b. It is free of atypical features encountered previously. Repeating the procedure for a series of true wind speeds v_T leads to a family of polar plots shown in the figure 11.

XVI. PRESENTING FULL PERFORMANCE

Constructed VPP produces much more information than can be read from a polar plot. For example, the RPY angles and position of the sailor are of high significance, but cannot be presented this way. To solve this problem, polar plots can be extended as follows. A single point (v, φ) gets replaced by a three dimensional miniature of the unit during sailing with speed v and true wind angle φ. Figure 12 shows the result of this idea. Red mark corresponds to the origin ($v = 0$ point) and red arrow represents the true wind. Both lengths and velocities can be read from the extended polar plot, so some characteristic time t is need to convert speed v to a representative distance on the plot vt. Here $t = 1.5\,\mathrm{s}$. Used sail shape was generated by a mathematical formula, designed to reconstruct qualitatively its characteristic.

XVII. ABSOLUTE OPTIMIZATION

The strategy used for optimizing additional state variables can be used to maximize any quantity q. First, we treat it as a parameter to the system of nonlinear equations and whenever they are solvable, q should be increased by sufficiently small Δq. This procedure is repeated until the maximal value $q_{\max}$ is obtained, past which no solution can be found. By "absolute optimization" we understand such setting of the gear that the overall course racing performance is possibly the best. Quantity q corresponding to this task should be an average of speed projected on the axis of the course (which is assumed to coincide with the true wind direction), which we denote by v_{eff}. Let v_U be the speed for the optimal upwind angle φ_U. Similarly, let v_D stand for the speed for the optimal downwind angle φ_D. Then:

$$v_{\text{eff}} = \frac{2}{\frac{1+b}{v_U \cos\varphi_U} - \frac{1-b}{v_D \cos\varphi_D}} \tag{46}$$

$v_U \cos\varphi_U$ and $-v_D \cos\varphi_D$ are velocities made good for upwind and downwind respectively. Thus for $b = 0$, v_{eff} is a harmonic average of them. Usage of this type of average follows from the fact, that lengths of the upwind and downwind legs (measured in the direction of the true wind) are equal. b is a bias parameter. Setting it to a small positive value accounts for greater importance of beating to windward from the tactical point of view. $b = 1$ would mean that we are interested only in optimizing the upwind performance. If sailing in the bad air (turbulence due to other sailors) is easy to avoid, $b = 0$ is the best choice.

During absolute optimization, a system of twenty nonlinear equations has to be solved each time, because upwind and downwind course are considered simultaneously. Each of the 15 state variables has to appear in two versions (for example θ_{fU} and θ_{fD} for upwind and

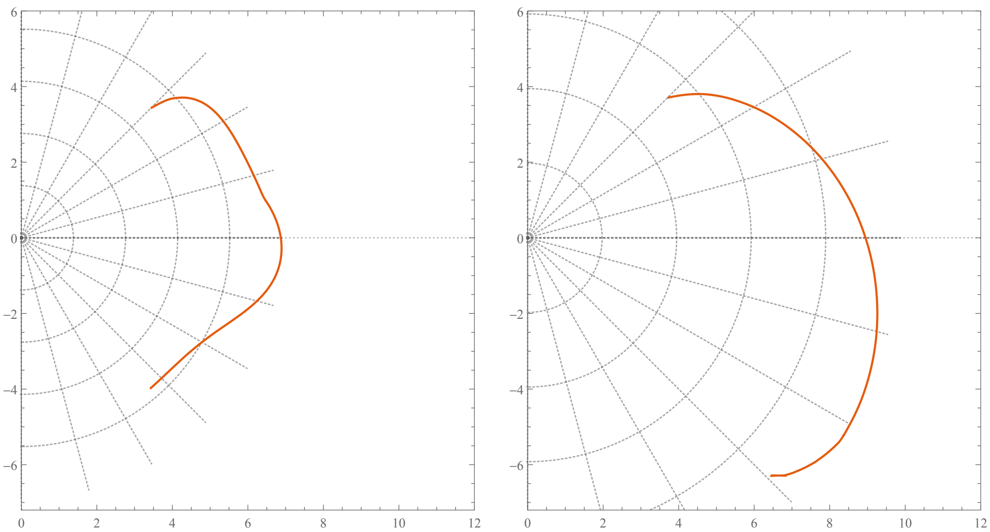

(a) without speed optimization over the additional state variables

(b) with speed optimization over the additional state variables

Figure 10: Polar plots generated for $v_T = 6\ \frac{\mathrm{m}}{\mathrm{s}}$. Speed is given in $\frac{\mathrm{m}}{\mathrm{s}}$.

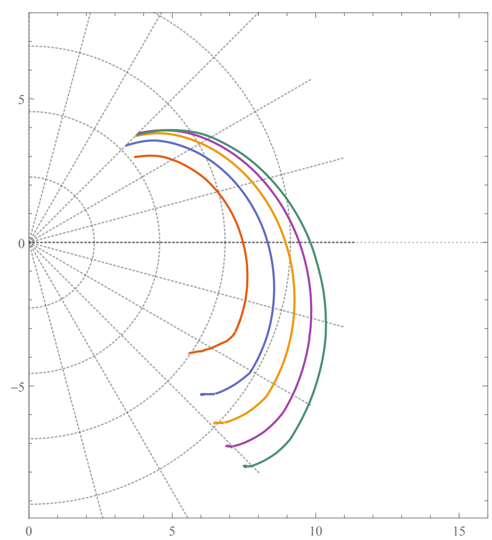

Figure 11: Polar plots generated for true wind speeds 4, 5, 6, 7 and 8 $\frac{\mathrm{m}}{\mathrm{s}}$.

downwind respectively). Additionally, we have to include φ_U and φ_D. This gives already 32 variables, to which we add all the equipment parameters we want to optimize (let n_{eq} be their number). Introducing the global parameter v_{eff}, we can get rid of one variable by means of equation (46). For example, we can substitute:

$$v_U = \frac{1+b}{\left(\frac{2}{v_{\mathrm{eff}}} + \frac{1-b}{v_D \cos\varphi_D}\right)\cos\varphi_U} \tag{47}$$

This gives $31 + n_{\mathrm{eq}}$ variables in 20 equations, which are solved for each v_{eff} update. Thus a thorough multi-parameter optimization may involve solving 20 equations for even twice that many variables. It is possible to impose constraints on some quantities in the VPP, like for example board width not greater than 100 cm.

Figure 13 shows the result of optimizing four equipment parameters: l_{eff}, x_{foot}, S_s and S_1 (front wing area was scaled together with the rear wing area). Initial values $l_{\mathrm{eff}} = 0.66\,\mathrm{m}$, $x_{\mathrm{foot}} = 1.25\,\mathrm{m}$, $S_s = 9\,\mathrm{m}^2$, $S_1 = 0.09\,\mathrm{m}^2$ have been tuned to $l_{\mathrm{eff}} = 0.647$ m, $x_{\mathrm{foot}} = 1.251$ m, $S_s = 9.003\ \mathrm{m}^2$, $S_1 = 0.0846\ \mathrm{m}^2$. First three were not modified considerably. Reduction of the front wing area is rather significant and its effect is exactly what foilers would expect. Downwind performance improved (both speed and angle), but for upwind sailing the speed got better at the expense of angle. However, overall outcome is positive. Gain of $\Delta v_{\mathrm{eff}} = 0.089\ \frac{\mathrm{m}}{\mathrm{s}}$ during a standard 12 min race gives an advantage of 64 m (in the direction of course axis), which corresponds to 13.4 s of time bonus. This optimization process has been conducted for $v_T = 6\ \frac{\mathrm{m}}{\mathrm{s}}$ and $m_{\mathrm{sailor}} = 67$ kg.

XVIII. LIMITATIONS AND FUTURE

Presented architecture of the VPP is very general and it is capable of taking in any CFD (or experimental) data. Its quality will be the main factor determining fidelity of the final results. There are, however, some simplifications built in the program itself. First of all, it neglects any interference between the modules, like for example effect of the board on the sail. This can be (to some degree) compensated by introducing effective values of some parameters (in this case it would be increased effective aspect ratio of the sail, which decreases $\mathcal{A}_s$). Of course depen-

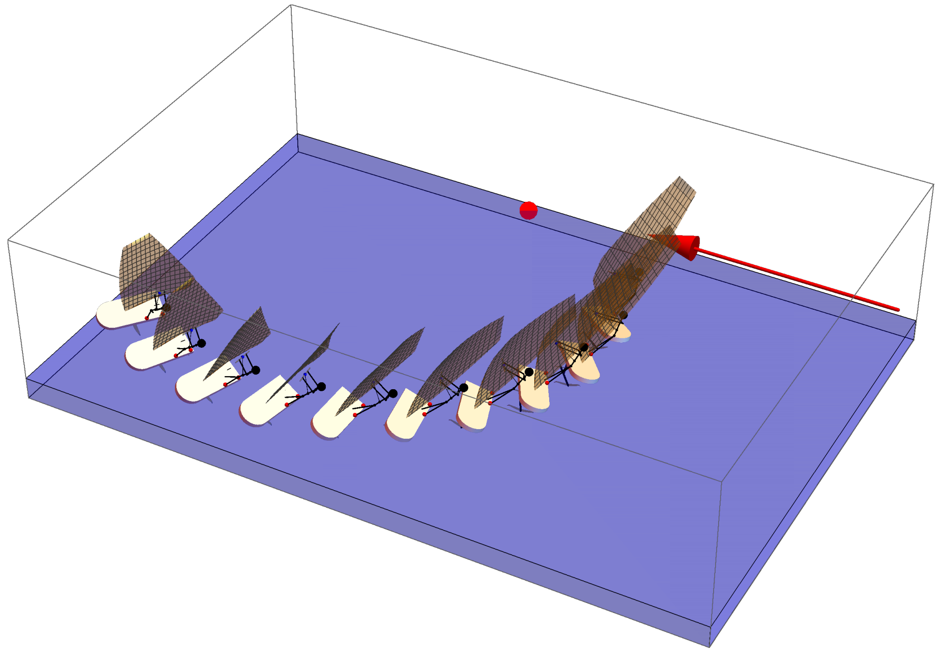

Figure 12: Extended polar plot shows the sailor in action on each possible course.

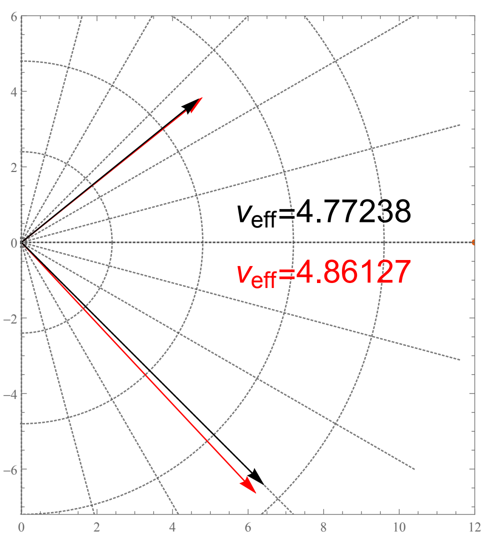

Figure 13: Red arrows represent enhanced upwind and downwind velocities. Black ones correspond to the initial setup.

dence of this effective aspect ratio on θ_f, ϕ_f, ψ_f cannot be accounted for. Secondly, the stick-man model, apart from its simplified nature, admits very unnatural positions. It can be eliminated by introducing constraints for β and F_2, but telling whether a certain position is comfortable (or at least rideable) for a real sailor is not easy. Next drawback is due to the complexity of nonlinear equations and multiplicity of parameters involved in the numerical methods (like the initial step Δv_{eff}, its minimal value and rate of reduction). It is good to supervise the program to control whether assumptions of the methods are met. One interesting feature is that time required for generating downwind part of the polars is significantly longer than that needed for the upwind part. The reason is not obvious (probably forces and torques vary more quickly in this region with the state variables).

Different sailing styles may require changes in the program. For example, sailors using fixed-length harness lines should treat l_{eff} as an equipment parameter, while for those using adjustable harness lines, l_{eff} becomes an additional state variable. Mast wetted height h_m is actually an additional state variable, but usually it is not regarded this way. Keeping the flight height precisely at given level is very difficult, so using an averaged value $h_m = \frac{1}{2}H$ has been used throughout the calculations.

Stability is not taken into account during optimization. It does not matter when optimized aspects weakly affect stability. However, if we pick two equipment parameters for optimization like the rear wing area and fuselage shift (relative to the foil mast), hydrodynamically most efficient setting has zero rear wing area and compensating fuselage shift. Of course, foil is unstable without the back wing. For this reason, suitable constraints have to be added by hand to avoid such situation.

The last important limitation concerns the steady-state assumption. For small and moderate waves, sailor does not have to react significantly to them. Crests are passed quickly enough, so their effect is smoothed by time-averaging. Of course, such situation requires appropriate CFD data including presence of the waves, but it does not seem to corrupt the steady-state assumption. When the wave height approaches H (roughly one meter), sailing becomes even a greater challenge. Sailor is forced to move back and forth periodically (especially downwind) and dynamic nature of the process is evident. Then a Dynamic Velocity Prediction Program may be needed.

Future development of the program will certainly consist in feeding it with realistic data (of a particular real-life gear to see effects of the optimization during races), adding automatic longitudinal stability constraints (and possibly rolling and directional too).

XIX. CONCLUSION

Constructed and described VPP is made of modules (parts responsible for different sub-problems like determining the force on the sail). The sailor position module uses a stick-man model to simulate three dimensional geometry of windsurfing. The program can be filled with CFD (or experimental) data as well with simple approximations. The last option has been used to produce qualitatively reasonable outputs. VPP can generate multiple polar plot curves for different true wind speeds 11, it can present details of the performance in three dimensions 12 and it is capable of multi-parameter constrained optimization of the equipment parameters 13. Future development of the program will certainly consist in feeding it with realistic data (of a particular real-life gear) to see effects of the optimization during races.

ACKNOWLEDGMENTS

I would like to thank my master and project supervisor Tomasz T. Polak, who has been motivating me to progress in physics for six years already. Also, my heartfelt appreciation goes to my dad – Marcin Urbański, who introduced me to the world of sailing and later windsurfing. Visualizing real life foiling in this paper would be impossible without permission and work of Rafał Czepułkowski (FotoSurf) – a photographer often present at Polish windsurfing foil regattas.

AUTHOR'S BIOGRAPHY

Oliwier Urbański is an undergraduate student of physics at Adam Mickiewicz University in Poznań. He is most fascinated with both condensed matter physics and physics of sailing. Training on windsurfing formula foil and participating in regattas is his favorite way of spending free time (after doing physics).

[1] J. Kimball, Physics of Sailing, Taylor and Francis Group (2010)

[2] K. Ernst, Fizyka Sportu, Wydawnictwo Naukowe PWN (2010)

[3] C. Marchaj, Aero-hydrodynamics of Sailing, Dodd, Mead & Company (1980)

[4] F. Eggert, Flight Dynamics and Stability of a Hydrofoiling International Moth with a Dynamic Velocity Prediction Program (DVPP), DOI: 10.13140/RG.2.2.20154.03524 (2018)

[5] S. F. Hoerner, Fluid-dynamic Drag, published by the author (1965)

[6] S. F. Hoerner, Fluid-dynamic Lift, second edition, published by the author (1985)

[7] M. Adolphe, J. Clerval, Z. Kirchof, R. Lacombe-Delpech, B. Zagrodny, Center of Mass of Human's Body Segments, Mechanics and Mechanical Engineering Vol. 21, No. 3 (2017) 485–497

[8] N. Sun, Homotopy Techniques in Solving Systems of Nonlinear Equations: A Theoretical Justification of Convex Combinations, Departmental Technical Reports (CS). Paper 864 (2014)

[9] E. W. Weisstein, Moore-Penrose Matrix Inverse, From MathWorld--A Wolfram Web Resource, `https://mathworld.wolfram.com/Moore-PenroseMatrixInverse.html`

[10] Y. Levin, A. Ben-Israel, A Newton Method for Systems of m Equations in n Variables, Nonlinear Analysis 47 (2001)